Noise reduction in support-constrained multi-frame blind-deconvolution restoration as a function of the number of data frames and the support constraint sizes
Journal Article (Postprint)

Charles L. Matson
Alim Haji

01 June 2007

Technical Paper

AIR FORCE RESEARCH LABORATORY
Directed Energy Directorate
3550 Aberdeen Ave SE
AIR FORCE MATERIEL COMMAND
KIRTLAND AIR FORCE BASE, NM 87117-5776

REPORT DOCUMENTATION PAGE

1. REPORT DATE *(DD-MM-YYYY)* 01-06-2007	2. REPORT TYPE Technical Paper	3. DATES COVERED *(From - To)* 01 Jan 2007 -01 Jun 2007

4. TITLE AND SUBTITLE

Noise reduction in support-constrained multi-frame blind-deconvolution restoration as a function of the number of data frames and the support constraint sizes Journal Article (Postprint)

5a. CONTRACT NUMBER
In-House DF701944

5b. GRANT NUMBER

5c. PROGRAM ELEMENT NUMBER
61102F

6. AUTHOR(S)

Charles L. Matson, Alim Haji

5d. PROJECT NUMBER
2311

5e. TASK NUMBER
S3

5f. WORK UNIT NUMBER
01

7. PERFORMING ORGANIZATION NAME(S) AND ADDRESS(ES)

AFRL/RDSA
3550 Aberdeen Ave. SE
Kirtland AFB NM, 87117-5776

8. PERFORMING ORGANIZATION REPORT NUMBER

9. SPONSORING / MONITORING AGENCY NAME(S) AND ADDRESS(ES)

Air Force Research Laboratory
3550 Aberdeen Ave. SE
Kirtland AFB NM, 87117-5776

10. SPONSOR/MONITOR'S ACRONYM(S)
AFRL/RDSA

11. SPONSOR/MONITOR'S REPORT NUMBER(S)
AFRL-RD-PS-TP-2008-1011

12. DISTRIBUTION / AVAILABILITY STATEMENT

Approved for Public Release; Distribution is Unlimited.

13. SUPPLEMENTARY NOTES

14. ABSTRACT

We show that the amount of relative noise reduction in multi-frame blind deconvolution image restorations is greatest for just a few data frames and is a more complicated function of the support constraint sizes.

15. SUBJECT TERMS

Image reconstruction-restoration; image enhancement

16. SECURITY CLASSIFICATION OF:			17. LIMITATION OF ABSTRACT	18. NUMBER OF PAGES	19a. NAME OF RESPONSIBLE PERSON Charles Matson
a. REPORT Unclassified	**b. ABSTRACT** Unclassified	**c. THIS PAGE** Unclassified	SAR	5	**19b. TELEPHONE NUMBER** *(include area code)* (505) 846-2049

Noise reduction in support-constrained multi-frame blind-deconvolution restorations as a function of the number of data frames and the support constraint sizes

Charles L. Matson and Alim Haji

Air Force Research Laboratory, 3550 Aberdeen Ave SE, Kirtland AFB, New Mexico, USA 87117-5776

Abstract: We show that the amount of relative noise reduction in multi-frame blind deconvolution image restorations is greatest for just a few data frames and is a more complicated function of the support constraint sizes.

1. Introduction

Multi-frame blind deconvolution (MFBD) algorithms seek to estimate jointly an object being imaged along with all the system point spread functions (PSFs) present in the measured data frames. It is well known that the quality of an object restoration improves as the number of data frames included in the restoration process is increased and as the support constraints used in the algorithm decrease in size (while still including the true support). This improvement is due to both a greater likelihood of finding the global minimum of the MFBD cost function (when a cost-function based approach is used, of course) and the decreased noise levels in the restored image. In this paper we report on results we have obtained while investigating the latter source of improvement. Our interest in exploring the amount of noise reduction as a function of the number of data frames and the support constraint sizes is due to a desire to better understand the tradeoff between improved image quality and increased algorithm execution time. We show that the amount of total noise reduction in the restored images is an increasing function of the number of data frames, and that the amount of relative noise reduction is greatest when adding including just a few data frames and is greater than might be expected. We define the term "relative noise reduction" in Section 3. We also discuss how the amount of relative noise reduction depends on the object and PSF support constraint sizes. Because we desire to obtain answers that are algorithm independent, we employ a Cramér-Rao lower bound (CRB) approach in the analysis. The outline of this paper is as follows: Section 2 contains a description of the imaging model and CRB theory, results are given in Section 3, and conclusions are presented in Section 4.

2. Imaging model and Cramér-Rao lower bound theory

The equation describing image formation is

$$i_m(\mathbf{x}) = h_m(\mathbf{x}) * o(\mathbf{x}) + n_m(\mathbf{x}) ; \quad m = 1,...,M \tag{1}$$

where $*$ denotes convolution, $\mathbf{x}$ is a two-dimensional spatial variable, $i_m(\mathbf{x})$ is the mth data frame, $h_m(\mathbf{x})$ is the mth PSF, $o(\mathbf{x})$ is the object being imaged, $n_m(\mathbf{x})$ is the mth noise realization, and bold-faced type denotes vectors and matrices. Because CRB theory requires a set of random variables, not stochastic processes, Eq.(1) must be rewritten in a vector form rather than as a continuous function. To this end, let α be a square grid of spatial locations of the intensity values of $i_m(\mathbf{x})$ and let $\mathbf{y}_m$, ψ, ϕ_m and η_m be one-dimensional vectors that contain the values of $i_m(\alpha)$, $o(\alpha)$, $h_m(\alpha)$, and $n_m(\alpha)$, respectively, on the grid defined by α. The vectors $\mathbf{y}_m$, ψ, ϕ_m and η_m can be generated from $i_m(\alpha)$, $o(\alpha)$, $h_m(\alpha)$ and $n_m(\alpha)$ by stacking their columns. In addition, let $\mathbf{H}_m$ be the block-circulant matrix associated with ϕ_m [1]. Then Eq.(1) can be rewritten as

$$\mathbf{y}_m = \mathbf{H}_m \psi + \eta_m \; ; \; m = 1,...,M \tag{2}$$

Multi-frame blind deconvolution algorithms seek to estimate jointly the parameters contained in the vectors ψ and $\{\phi_m\}$ given the data vectors $\{\mathbf{y}_m\}$, where the quantities in braces are the collection of vectors for all m. Although we could have carried out this analysis using sample statistics generated from restorations produced by a

specific MFBD algorithm, we desired to generate algorithm-independent results. Therefore, we chose to use CRB theory [2] for the analysis since it produces lower bounds to the variances of any unbiased estimates of a set of parameters. The CRBs for any unbiased estimates of the elements of the concatenated vector $\boldsymbol{\theta} = \left[\boldsymbol{\psi}^T, \boldsymbol{\varphi}_1^T, ..., \boldsymbol{\varphi}_M^T \right]$ are the diagonal elements of the inverse of $\mathbf{F}$, the FIM associated with $\mathbf{y}_m$ and $\boldsymbol{\theta}$. The element of $\mathbf{F}$ in the pth row and the qth column is given by

$$\mathbf{F}_{pq}(\boldsymbol{\theta}) = E\left[\frac{\partial \ln f(\mathbf{y};\boldsymbol{\theta})}{\partial \boldsymbol{\theta}_p} \frac{\partial \ln f(\mathbf{y};\boldsymbol{\theta})}{\partial \boldsymbol{\theta}_q} \right] \tag{3}$$

where f($\mathbf{y};\boldsymbol{\theta}$) is the probability density function of $\{\mathbf{y}_m\}$ parameterized by the vector $\boldsymbol{\theta}$ and ln denotes the natural logarithm. Equation (3) gives the elements of $\mathbf{F}$ for the imaging model of Eq.(2) without the application of any constraints. Support constraints are implemented by including in the vectors $\boldsymbol{\psi}$ and $\{\boldsymbol{\phi}_m\}$ only those elements that are inside their support constraint regions [3]. The unbiased CRBs of the parameters $\boldsymbol{\theta}$, CRB($\boldsymbol{\theta}$), are given by

$$\mathrm{CRB}(\boldsymbol{\theta}) = \mathrm{diag}(\mathbf{F}^{-1}) \tag{4}$$

where diag($\mathbf{F}^{-1}$) denotes a vector containing the diagonal elements of $\mathbf{F}^{-1}$. Because of the scaling redundancy of blind deconvolution, this expression for $\mathbf{F}$ is non-invertible. We make $\mathbf{F}$ invertible by estimating only N-1 elements of $\boldsymbol{\psi}$ and N_m-1 elements of $\{\boldsymbol{\phi}_m\}$, where N and N_m are the numbers of pixels in the support constraints applied to these vectors, and by requiring that all the $\mathbf{H}_m$ have full rank, which occurs when the Fourier transforms of $\{h_m(\boldsymbol{\alpha})\}$ are non-zero.

3. Results

We calculated CRBs using the object in Fig.1 for o($\mathbf{x}$) and zero mean white noise with variance σ^2 for $n_m(\mathbf{x})$. The PSFs $\{h_m(\mathbf{x})\}$ are related to atmospheric PSFs for D/r_o = 8, where D is the telescope diameter and r_o is the atmospheric correlation length [4]. We created $\{h_m(\mathbf{x})\}$ by creating D/r_o = 8 PSFs, Fourier transforming them, cutting out a square portion of this Fourier transform centered at zero frequency and contained within the telescope OTF support, and then inverse Fourier transforming the results. The resulting $\{h_m(\mathbf{x})\}$ are invertible, making $\mathbf{F}$ invertible. We chose to do this to avoid the complications of calculating and interpreting biased CRBs.

   A plot of the unbiased CRBs for $\boldsymbol{\psi}$, $\mathrm{CRB}_M(\boldsymbol{\psi})$, normalized to one for M=1, is given in Fig. 2 as a function of the number of data frames M included in the MFBD process. For this plot, the true object support was used for $\boldsymbol{\psi}$ and a circular support that contained more than 99% of the energy of the $\{h_m(\mathbf{x})\}$ was used. For each M, the corresponding point in the plot is the sum of $\mathrm{CRB}_M(\boldsymbol{\psi})$, denoted sum($\mathrm{CRB}_M(\boldsymbol{\psi})$). Notice that sum($\mathrm{CRB}_M(\boldsymbol{\psi})$) is a decreasing function of M, as expected. Simplistically, one might expect sum($\mathrm{CRB}_M(\boldsymbol{\psi})$) to decrease as 1/M since the noises are statistically independent from frame to frame. This 1/M behavior is present, for example, when using speckle imaging techniques to estimate the energy spectrum of an object [4]. To investigate this expectation, we plotted the function 1/M in Fig. 2 as well. Notice that the sum($\mathrm{CRB}_M(\boldsymbol{\psi})$) plot decreases more rapidly than 1/M for small values of M. We refer to the magnitude of the slope of sum($\mathrm{CRB}_M(\boldsymbol{\psi})$) as the amount of relative noise reduction. This implies that MFBD image restorations benefit more than might be expected from adding just a few frames to the estimation process as compared to carrying out blind deconvolution using only one data frame. We have seen this behavior in restorations obtained using field data as well. Notice also that the slopes of the sum($\mathrm{CRB}_M(\boldsymbol{\psi})$) plot and the 1/M plot appear to be equal for larger values of M. This means that the expected 1/M relative noise reduction in the restored images occurs for larger values of M.

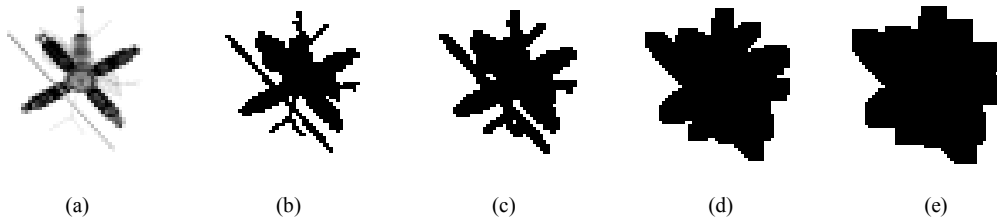| | | | | |
| (a) | (b) | (c) | (d) | (e) |

Fig. 1. Computer-simulated satellite model (a), and support constraints used for CRB calculations: (b) true, (c) blur2, (d) blur 5, and (e) blur 7.
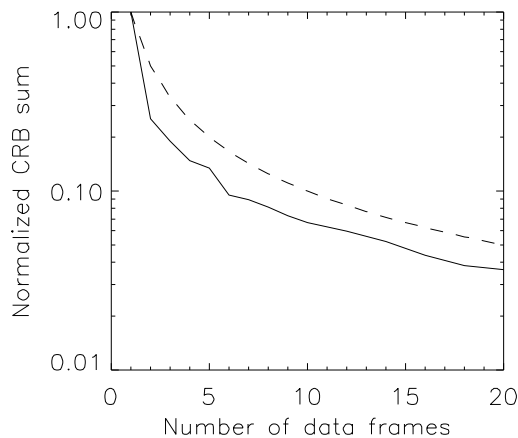
Fig. 2. Plots of the normalized sum($CRB_M(\psi)$) values (solid line) and $1/M$ (dashed line) as a function of M
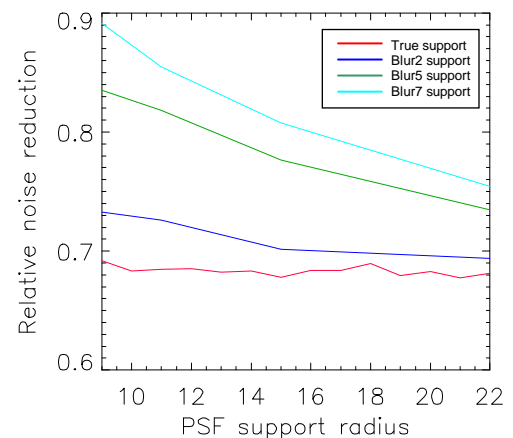

Fig. 3. Amounts of relative noise reduction when adding a second frame, as a function of object and PSF support sizes.

We then investigated how the amounts of relative noise reduction that occur in sum($CRB_M(\psi)$) as a result of using two (M=2) instead of one (M=1) frames of data depend on the object and PSF support constraint sizes. To do this, we calculated sum($CRB_2(\psi)$) for several object and PSF support constraints. We used four different object support constraint sizes: the true support region and three larger support regions created by blurring the true support region with 2 x 2, 5 x 5, and 7 x 7 blurring kernels (see Fig. 1). The PSF supports were all circular with varying radii. The amounts of relative noise reduction are displayed in Fig. 3, where a value of zero indicates no additional noise reduction and a value of one indicates complete noise removal achieved with the use of the second frame. Notice that the amounts of relative noise reduction are a decreasing function of the PSF support radius for all blurred object support constraints, but are independent of the PSF radius for the true object support case. Notice also that the benefit of adding a second frame to the MFBD process increases as the object support constraint size increases for a fixed PSF support constraint size. This second property is especially useful since highly-accurate object supports are difficult to generate, in general. We note that the amount of relative noise reduction corresponding to a $1/M$ reduction is 0.5 for M=2.

We emphasize that the results in Fig. 3 are based on the normalized sum($CRB_M(\psi)$) values, not the absolute values. Without this awareness, the results in Fig. 3 could be interpreted to mean that a less-accurate object support constraint produces lower CRB values than does a more-accurate object support constraint, which is not true. The proper conclusion to draw is that noise reduction occurs more swiftly as M increases for less-accurate support sizes.

4. Conclusions

Using an algorithm-independent CRB approach, we have analyzed the amount of noise reduction possible when using MFBD algorithms. We investigated the amount of absolute and relative noise reduction as a function of the number of data frames included in the restoration process and the sizes of the object and PSF support constraints. We showed that the relative noise reduction is greater than $1/M$ for values of M on the order of one, where M is the number of data frames, and is approximately equal to $1/M$ for larger values of M. We also showed that the amount of relative noise reduction achieved for M = 2 is generally an increasing function of object support constraint size. For all but the true object support constraint case, the amount of relative noise reduction is a decreasing function of the PSF support size.

5. References

[1] R. C. Gonzalez and R. E. Woods, *Digital Image Processing* (Addison-Wesley, Reading, MA, 1992), Chap. 5.
[2] B. Porat, *Digital Processing of Random Signals, Theory and Methods* (Prentice-Hall, Englewood Cliffs, NJ, 1994), Chap. 3.
[3] J. D. Gorman and A. O. Hero, "Lower bounds for parametric estimation with constraints," *IEEE Trans. Inf. Theory* **26**, 1285-1301 (1990).
[4] M.C. Roggemann and B. Welsh, *Imaging Through Turbulence* (CRC Press, Boca Raton, FL, 1996).